10 Inertial confinement fusion: heavy ions

[R.M. Bock, I. Hofmann, D.H.H. Hoffmann, G. Logan]

10.1 Introduction

Concepts of inertial confinement fusion (ICF) are based on the fact that lasers (Chap. 8), z-pinches (Chap. 9), and ion beams offer the opportunity to concentrate energy in matter at an extremely high density on a very short timescale. In this chapter it will be shown how beams of heavy ions interact with matter and how they can be used to compress and ignite DT-filled pellets for the generation of fusion energy. Different from the surface absorption and strong reflection of laser beams, beams of energetic heavy ions, such as lead or bismuth, are stopped in matter in a thin layer and deposit there the total amount of kinetic energy. By the high energy density produced, the pellet is compressed by ablation and, at the phase of stagnation, the fuel is ignited and burned. As compared to beams of protons and light ions, heavy ions offer the advantage of about hundred times higher energy deposition. Another specific benefit in using heavy ions is their efficient acceleration, their classical behavior in beam transport, and the concentration of high beam power into small beamspots.

The target, its preparation and structural composition, its dynamical behavior during compression and burn, and the requested driver and beam properties have been presented and discussed for laser beams and z-pinches in Chaps. 8 and 9, respectively. Many of these facts and relations, in particular the dependence of energy gain on the deposited energy, are valid for heavy ion beams as well. Here, we will concentrate on the characteristic features of heavy ions and will present some specific results of ion-plasma interaction which provide the basis for theoretical predictions by computer simulations. Target technology, too, has continuously made progress in the last decades, in particular the production, as well as filling and layering procedures, and remarkable precision has been achieved. All these achievements greatly contribute to the final aim of inertial fusion. One has to keep in mind, however, that ignition and burn have not been demonstrated yet by experiments, and most of our present knowledge about the target performance and target gain is based on theoretical models. Section 10.2 will be devoted to the interaction of beams with cold matter and plasmas, and to specific issues of heavy ion targets.

For the design of a driver facility, for accomplishing an efficient acceleration and the necessary excellent beam quality, a highly developed accelerator technology is available as well as an experience of more than four decades of research in nuclear and high-energy physics with very sophisticated and continuously improved accelerator facilities. The requirements for the fusion driver, however, are still beyond present accelerator performance and need further research on specific issues. In particular, beam dynamics near the space charge limit is an important feature in this context. Nearly all of these problems are well understood on a theoretical basis, but more experimental investigations are necessary. Some of the powerful new accelerator projects now under consideration are aiming at high-intensity heavy ion beams and will provide useful information on critical issues of high-intensity acceleration. Two complementary accelerator concepts for the design of a reactor driver are pursued by the inertial confinement energy (IFE) community and will be presented in Sect. 10.3

Compared to magnetic confinement fusion, the inertial fusion reactor concept has some intriguing features: Because of the spatial separation between driver and reactor chamber, there is much more freedom for specific issues of chamber design. The inertial fusion reactor offers the realization of a thick-liquid wall for cooling, breeding and first-wall protection. This shielding against radiation will improve operation and maintenance of the reactor plant, and its lifetime will be increased considerably. From the research and design work of the last three decades it is obvious that the inertial fusion reactor has favorable properties, also concerning safety and environmental problems. Section 10.4 will give an overview on recent activities in this field.

10.2 Target physics

10.2.1 Interaction of heavy ions with matter

Interacting with intense heavy ion beams the target material generally consists of a mixture of electrically charged ions, electrons, and neutral particles. In this situation, collective effects determine the statistical properties of the sample. Atoms and ions immersed in a plasma environment experience perturbations from the plasma. As a result the atomic and ionic states turn out to be mixed and are strongly different from pure, unperturbed atomic states. They are also different from those in a cold matter environment. Consequently, not only the spectral characteristics of radiation emission and absorption by the atoms and ions are substantially different from spectra of the unperturbed species, but also bulk matter properties. These can be expressed in terms of an equation of state, relating pressure and temperature to the matter density of the sample, and also by the electrical and thermal conductivity, and radiation transport properties. In general, these properties turn out to be vastly different from those of matter under ordinary conditions.

Heavy ion beam scenarios for IFE have to take into account the specific properties of ion beams and their energy deposition characteristics in both cold and ionized matter. A schematic comparison of heavy ion beam and laser energy deposition properties is shown in Fig. 10.1. Due to their mass, heavy ions at high kinetic energy are very efficient carriers of energy. Moreover, the accelerating mechanisms in heavy ion accelerators are also very effective to convert RF or pulsed induction energy into kinetic energy of heavy ions. Heavy ion beams deposit their energy inside the target volume, whereas laser beams are absorbed close to the surface.

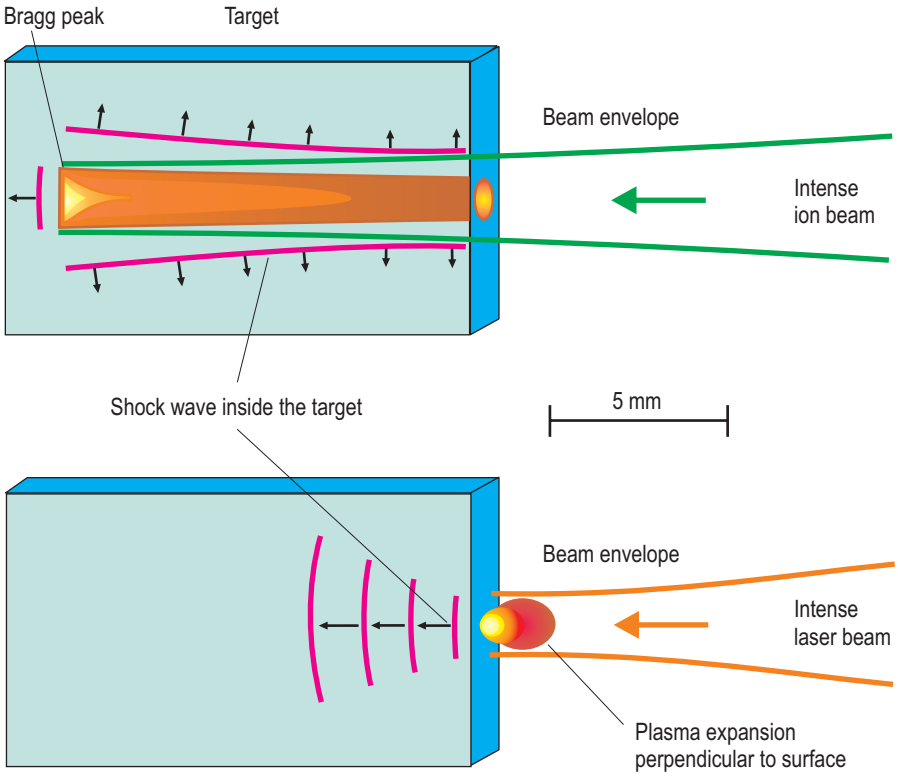

Fig. 10.1. Schematic comparison of the energy deposition of an intense heavy ion beam and that of a high-performance laser in a solid target. Ion beams penetrate deep into the material whereas laser beams are absorbed only below the critical density n_c, where the plasma frequency ω_p of the material is smaller than the laser frequency ω_l.

The specific energy deposited in the target material, E_s, can be related to the energy deposition of energetic heavy ions in matter, dE/dx, the matter density, ρ, the particle number of the beam bunch, N, and the focal spot, πr^2, as follows:

$$E_s = 1.6 \times 10^{-19}\, N\, (dE/\rho dx) / (\pi r^2) \qquad \text{(unit: J/g)}. \tag{10.1}$$

In this way heavy ion beams couple their kinetic energy in a very efficient way to the target material. Since the stopping power depends strongly on the charge state of the ion, the heaviest ions deposit the maximum energy density in matter, as shown in Fig. 10.2. In an ICF concept where the fusion capsule is directly irradiated by the ion beam ("direct drive"), this energy coupling mechanism may turn into a disadvantage, since irradiation or material inhomogeneities imprinted onto the capsule may lead to a decreased robustness against Rayleigh-Taylor instabilities. Until now no efficient transport mechanisms to smoothen these initial inhomogeneities in a direct drive scheme are known. This is still a topic of current research, and a possible cure depends on the detailed knowledge of material properties such as the equation of state and transport properties at high energy density conditions.

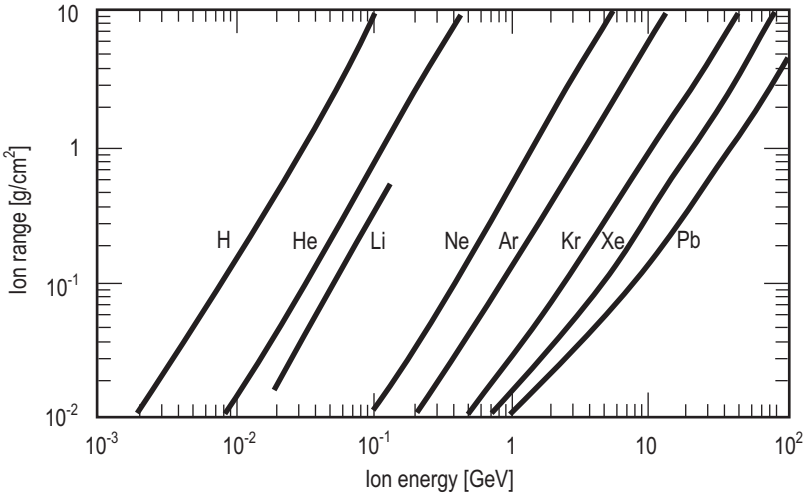

Fig. 10.2. Range-energy relation for protons and various heavy ions. Since the thickness of the surface layer of a pellet in which the energy is deposited is fixed by an optimized compression dynamics, the heaviest ions are best suited.

So far as has been observed, heavy ion beam stopping is governed by classical beam energy loss collisions with the target electrons and ions. No collective beam-plasma instabilities have been found to be important in heavy ion beam stopping in dense target plasmas. Interaction processes of heavy ions with ionized matter at high energy density, like energy deposition and charge-changing cross sections, are known to be considerably different from those with cold matter and may change by more than one order of magnitude [95Jac, 94Hof]. Only for a few cases, where the plasma is ideal and fully ionized, experimental data exist and can be explained within the framework of a modified Bethe-Bohr-Bloch stopping theory. One example is shown in Fig. 10.3, where the upper curve represents the energy loss data of high-energy lead ions in a fully ionized hydrogen plasma target as a function of the plasma line density. The target was 20 cm long and the plasma free-electron density above 2.5×10^{19} cm^{-3} during the pinch phase of a z-pinch plasma. Energy loss data for the same situation in a hydrogen gas are shown in the lower curve of Fig. 10.3. The difference in stopping power is even more pronounced at lower beam energy where an enhancement factor of approximately 40 was measured for stopping in ionized matter as compared to cold matter [95Jac].

For dense, non-ideal, and partially ionized plasma the experimental and theoretical data base is only starting to develop. The physics of such dense and strongly coupled plasmas is closely related to those states of matter at high energy density and high pressure above 1 Mbar.

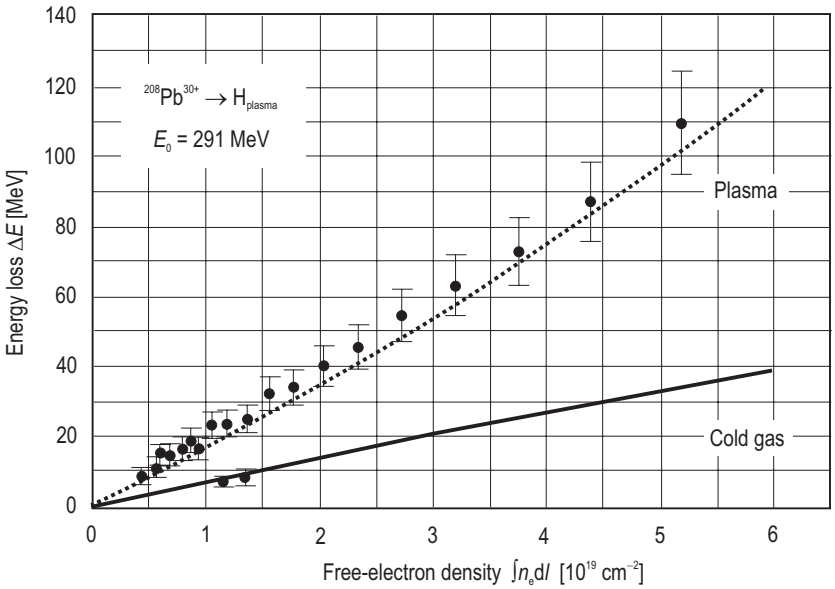

Fig. 10.3. Energy loss of lead ions in cold hydrogen gas and fully ionized hydrogen plasma, respectively. The enhanced energy loss in plasma is due to a higher effective charge state of the ions traversing ionized matter and more effective energy transfer in collisions with free electrons.

10.2.2 Basic issues of IFE target development for heavy ion beams

A necessary condition to achieve ignition and high gain is the irradiation symmetry of the pellet. Due to the efficient energy coupling and transfer mechanisms of heavy ions to the target material, irradiation asymmetries may be generated right at the initial phase of ablation and compression. This is especially true for a low number of beams, where the symmetry requirement is difficult to achieve in a *direct drive* scheme, already for principal geometric reasons. In an *indirect drive* scheme, first proposed at Livermore in 1993 [93Lin], the spherical fusion capsule is enclosed by a cylindrical casing in which the heavy ion beam energy is changed by two converters on opposite sides into soft X-ray radiation inside the casing (hohlraum radiation). The spherical fusion capsule is radiatively imploded by the much more symmetric hohlraum radiation. Since this scheme was proposed, many different approaches to indirectly driven targets have been investigated. This has recently been summarized in [02Cal, 02Bas]. It is of fundamental interest whether the introduction of additional shine shields inside the casing may lead to the necessary radiation symmetry. Figure 10.4 shows an example where the introduction of a varying number of radiation shields inside the casing can reduce the radiation asymmetry below the required level of approximately 1 % [97Mar].

Since a two-sided illumination of the target seems to provide the most suitable irradiation symmetry for intense heavy ion beams, it is necessary to convert the ion beam energy into radiation and distribute it into almost 4π steradians surrounding the implosion capsule. In the example shown in Fig. 10.4, radiation shields are used with sufficient success. A different concept was suggested by Tabak and Callahan-Miller [98Tab, 99Cal, 00Cal], where the converter target is distributed in solid angle to achieve the desired radiation symmetry. The case-to-capsule ratio is, of course, an important number which affects the energy gain of the fusion pellet. Two-dimensional integrated calculations show, however, that for an optimized heavy ion target a gain of 130 can still be achieved in a close-coupled version of the distributed radiator target. Optimized high-gain targets have been designed and investigated by a number of research groups [88Ram, 99Vat] contributing to the *European Study Group on Heavy Ion Driven Inertial Fusion* (*HIDIF*) [98HID].

The effort to optimize the case-to-capsule ratio has the effect that the resulting hohlraum geometry tends to become smaller. Therefore, the demands on the final beamspot are also increasing and the demands on final focusing, space charge neutralization in the reactor chamber, beam transport and emittance growth in the accelerator increase likewise. A more specific approach for an indirect drive target will be presented in Sect. 10.3.

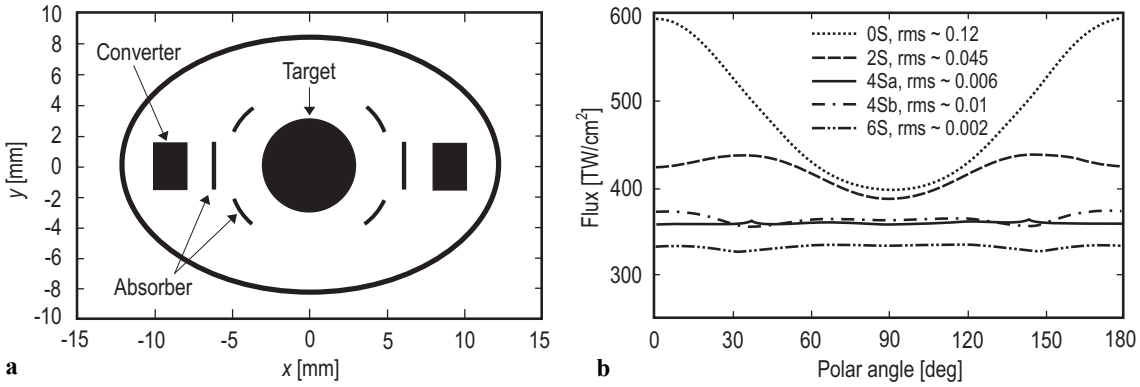

Fig. 10.4. **(a)** For a two-sided target illumination it is necessary to introduce shine shields between the converter target and the pellet. **(b)** Simulation results [97Mar] of radiation fluxes onto the pellet versus polar angle, showing that this additional shielding can reduce the radiation asymmetry to the required level.

10.2.3 Physics of dense plasmas and fast ignition

For the design of an efficient IFE target with high gain, the basic processes of beam-plasma interaction and the hydrodynamic response of matter need to be understood on a microscopic level. The detailed knowledge of heavy ion energy deposition in a target that is partly ionized and in a state of high energy density is obviously a prerequisite for the design of the target as well as for realistic simulations of target hydrodynamics. With the facilities available now, the regime of hydrodynamic expansion of beam-heated matter can be investigated. However, for experiments to measure the conversion of kinetic beam energy into radiation, in the regime of radiation-dominated plasmas, the available intensity of heavy ion beams is not sufficient. Laser facilities, such as the *PHELIX Laser Project* at GSI [98PHE], combined with the new *Heavy Ion Synchrotron Facility FAIR* to be built in the next decade, will allow beam-plasma interaction phenomena in high-density, high-temperature plasmas to be addressed [01Hen].

Already in 1994 a new concept for the ignition of an inertial fusion target was proposed [94Tab]. The new scheme is known to the community as *Fast Ignition* and allows igniting a fusion target with a considerably reduced amount of energy for the primary driver beam [98Mey]. The usual concept of ignition as shown in Fig. 10.5 is based on spherical compression to form an ignition spark in the center of the shock-compressed fuel. From this spark area a propagating burn wave is launched and propagates throughout the fuel. Fast ignition is based on the idea to decouple the compression and ignition process. As shown in Fig. 10.5, the fuel is first compressed in a standard way by the power of an intense heavy ion beam. Ignition is then independently achieved in a separate process. Early discussions about fast ignition involved an external laser pulse of ultra-short duration and extremely high intensity [96Puk]. In this case the beam has to propagate through over-dense plasma, which is a regime where the plasma frequency corresponding to the plasma density is higher than the laser frequency. Classically an electromagnetic wave cannot propagate under these conditions. Interaction processes of the ultra-short high-intensity laser beam will create a relativistic electron beam which travels towards the highly compressed fuel core.

The physics of this process is not yet fully understood, but experimental as well as theoretical investigations worldwide are addressing this problem vigorously, since laser beams with intensities exceeding 10^{19} W/cm^2 are available now with the advent of ultra-intense short-pulse lasers [00Sna]. Recent experiments have also demonstrated that such laser beams impinging on a curved target surface can create a high-energy intense proton beam [01Rot], which can be used to propagate towards the highly compressed fuel and finally ignite it. The scenario illustrated in Fig. 10.6 combines all ICF schemes that have been treated separately. The power of highly efficient heavy ion beams is converted to radiation in the converter targets of a hohlraum. The hohlraum is heated up to a temperature that can be much lower than in conventional hohlraums to compress the pellet inside the hohlraum. During the final stage of the process, an ultra-short high-intensity laser pulse is fired towards the hohlraum casing producing an intense beam of protons that propagates to the compressed fuel core and achieves ignition. In this scenario Laser Fu-

sion, Light Ion Beam Fusion, and Heavy Ion Beam Fusion finally unite into one scenario. The next decade will probably see a breakthrough in the physics of inertial fusion based on the development of ultra-short lasers combined with intense particle beams.

10.2.4 Conclusions

Inertial fusion energy with heavy ion beams is an area of active basic research while some aspects are already technically feasible. Currently the two big laser facilities under construction in the US and in France are the main projects towards inertial fusion. Heavy ion laboratories such as GSI Darmstadt are continuously increasing the heavy ion beam power for experiments. With a high-power laser beam from the PHELIX laser and the intense heavy ion beam, key issues of high energy density physics can be addressed to study the properties of matter under extreme conditions of temperature and pressure. A major development is the upcoming of ultra-short pulse lasers in recent years. The detailed knowledge about interaction phenomena of intense fields with matter will certainly also influence the development towards inertial fusion. As pointed out the fast-igniter scenario holds the prospects of combining the advantages of lasers, light ions and heavy ion beams into one IFE scheme. It reduces the demands on the accelerator with respect to the total beam energy to be delivered to the target.

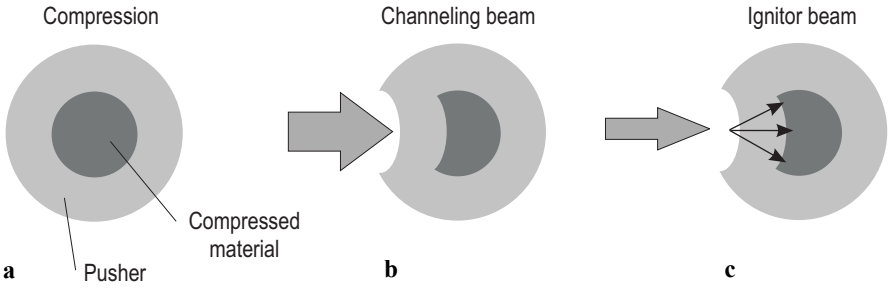

Fig. 10.5. Schematic concept of fast ignition. In step **(a)** the fuel is compressed in the standard way by high-power beams, however, with lower requirements on spherical symmetry. A channeling beam **(b)** is then used to drill a hole into the dense plasma environment, and in **(c)** the power of an ultra-short high-intensity laser pulse is converted into a particle beam penetrating towards the dense core where the compressed fuel is finally ignited.

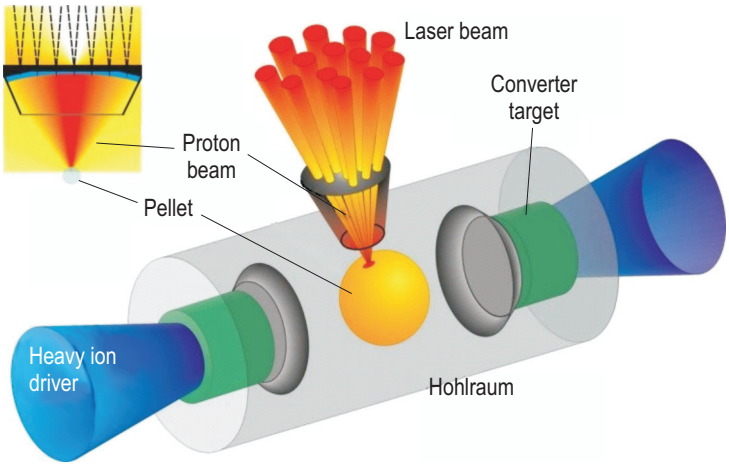

Fig. 10.6. Indirectly driven fast ignition using heavy ions, laser beams and laser-accelerated proton beams. The dimensions are not to scale. The surface of the laser target is shaped to focus the ion beam into the spark volume [01Rot].

10.3 Heavy ion driver concepts

10.3.1 Introduction

Heavy ion accelerators for ICF have been considered since the mid-1970s [76Mas] as a promising alternative to the already more established paths towards fusion energy production. Specific benefits in using heavy ion beams are efficient acceleration, classical behavior in beam transport, favorable focusability of high-energy heavy ion beams, and excellent beam-target coupling. Moreover, the highly developed technology of proton and ion accelerators for high-energy and nuclear physics with at least 50 years of experience can be used. These accelerators have proven to be reliable and with high efficiency and repetition rate [94Boc]. High average power proton accelerators – generating typically 1 MW power with high repetition rate – are under construction as drivers for spallation neutron sources and other applications: The SNS at Oakridge/USA [03Hol], and the JPARC facility in Japan [02Yam]. The primary development goal in heavy ion fusion (HIF) is to demonstrate that the extremely high peak power needed for target compression and ignition can be achieved with accelerators. Such high peak power is the proven strength of laser facilities for ignition experiments. Laser technology, on the other hand, faces the well-known technical difficulties to generate the high average power needed for commercial energy production. While heavy ion accelerators cannot compete with lasers for single shot experiments or ignition, they should be viewed as a technology with a high potential for later application in the commercial use for energy production.

Two complementary accelerator scenarios are considered as potential inertial fusion drivers:

(1) The *RF linac & storage ring* approach, which benefits from large experience with existing linear accelerators and storage rings. It has been in the focus of two system studies coordinated by GSI Darmstadt, the HIBALL study in 1980-84 [81Bad, 83Boc, 85Bad], and the HIDIF study in 1998 [98HID].
(2) The *induction linear accelerator* concept has been developed in the United States. A dedicated experimental program with key experiments in acceleration, transport and focusing is pursued in the VNL (Virtual National Laboratory) for Heavy Ion Fusion, in a joint effort by LBNL, LLNL and Princeton University [02Log].

10.3.2 Basic principles

10.3.2.1 Requirements for fusion energy production

Target parameters suitable for heavy ion drivers are not significantly different from those of laser drivers, although different optimizations may be needed. The driver efficiency and the actual energy gain of the target play an important role for the driver performance. A reasonable ratio between circulating energy and thermal energy output from the reactor can be reached only by sufficiently large driver efficiency. For a given target gain, reducing the driver efficiency from 25 % to 5 %, for example, would increase the recirculating power from 12 % to the unacceptably large value of 60 %. An efficiency of 20…25 % can be reached with conventional accelerator technology used in high-energy physics for protons or heavy ions as was demonstrated in the HIDIF study [98HID].

A typical assumption in heavy ion system studies has been to use a target gain G of 80…100, which is confirmed by different gain models. Extensive code simulations have indicated that such a gain should be possible with an input energy of 5 MJ under "conservative" assumptions on entropy increase and hydrodynamic coupling efficiency during the implosion. For effective compression this energy has to be delivered during 10 ns, which sets the standard power requirement for the accelerator driver to the value of 500 TW. In principle, there is a bandwidth of possible ion currents and kinetic energies to match this condition. For heavy ions with mass $A \approx 200$, a reference value for an optimum kinetic energy is 10 GeV. To reach the power of 500 TW necessary for ignition, a total particle current of 50 kA is a typical requirement. In order to fulfill this requirement with protons the corresponding numbers would typically be

10 MeV for the kinetic energy and 50 MA for the total beam current. This was studied in the context of pulsed power technology for which the issues of repetition rate and reliability have remained basically unresolved.

More important than the total power is, however, the specific power, P, which measures the power delivered per unit mass and thus determines the actual temperature and pressure rise in the target beam stopper:

$$P = (E \cdot I)/(R \cdot F) \,, \tag{10.2}$$

where E is the total kinetic energy, I is the particle current, R denotes the range (in g/cm^2), and F (in cm^2) is the focal spot area. In most studies, ranges between 0.1 and 0.3 g/cm have become standard, although still shorter ranges and lower energies would be preferable. The specific power required to achieve 300 eV plasma temperature in the target is estimated as $P = 10^{16}$ W/g [92Mey], which clearly gives preference to small range, hence low kinetic energy and heavy ions. For heavy ions the range is basically a result of classical Coulomb stopping, and anomalous effects are expected to be absent.

10.3.2.2 Intense heavy ion beams

Besides the preference for heavy ions the optimum choice of the kinetic energy is still open. It can be narrowed down by requesting vacuum transport in the accelerator as well as from the accelerator to the reaction chamber and target, which calls for not too low energies.

A crucial issue is the possibility to transport and focus the heavy ion beams within the different accelerator structures and between the accelerator and the target with appropriate focusing to prevent the beam from diverging due to its emittance and space charge. Maschke formulated a current limit for beam transport in vacuum with quadrupole lens focusing [79Mas]. It can be expressed as:

$$I_0 = 1.8 \times 10^6 \, (A/Z)^{1/3} \, B_0^{2/3} \, (\beta\gamma)^{5/3} \, \varepsilon_N^{2/3} \,. \tag{10.3}$$

Here, I_0 is the electrical current, A and Z the atomic mass and the charge state of the ion, B_0 denotes the pole tip field (precisely, the magnetic field at the maximum beam radius), and ε_N is the normalized emittance (= $\varepsilon\beta\gamma$, where the emittance ε is the product of beam radius and divergence, and $\beta = v/c$ and γ are the relativistic factors). The physics behind this limit is the assumption that the repulsive beam space charge force just balances 75 % of the externally applied focusing force. This value is a reference value – it can even be exceeded as was shown by theory and experiment with a Cs^+ beam in a long quadrupole channel consisting of 41 lattice periods [84Chu, 86Kee], provided that so-called "transport instabilities" are avoided [83Hof1, 83Hof2]. Equation (10.3) is applied to the final transport from the accelerator to the reactor and the target, both in the RF linac & storage ring as well as in the induction linac scenarios. In both scenarios it must be considered during the final bunch compression process prior to extraction. As an example: For 10 GeV ions with $A = 200$ ($\beta = 0.3$), $Z = 1$, $B = 4$ T, and $\varepsilon = 10^{-5}$ mrad, we obtain typical currents of 1 kA per transport channel. On this basis the number of beamlines to the target chamber is estimated as 50; in detailed designs it can be larger if symmetry requirements of target illumination are more stringent. Equation (10.3) also allows estimating the current limit at all energies of an induction linear accelerator and shows that higher peak currents can be accelerated at increased energies, hence simultaneous bunch length reduction ("bunch compression") is allowed with increasing kinetic energy.

Equation (10.3) favors high atomic mass and also high kinetic energy, since the current scales like $I_0 \sim E^{5/6}$, and the beam power like $T \sim E^{11/6}$, where E is the kinetic energy. This scaling demonstrates that the highest kinetic energies would be desirable as they lead to a smaller total number of beams on target. This is opposite to the preference for relatively low kinetic energies for the target requirements as suggested by the dependence of the stopping range on kinetic energy. A compromise between both leads to practical ion energies of 5…10 GeV. Typical accelerator parameters for an indirectly driven target are summarized in Table 10.1.

Table 10.1. Typical accelerator and target parameters.

Ion species	$^{209}Bi^{1+}$
Kinetic energy	10 GeV
Total energy	5 MJ
Final pulse duration	10 ns
Final momentum spread	3×10^{-3}
Emittance at target	20 mm mrad
Spot radius	3 mm
Ion range	0.3 g/cm^2
Specific power	10^{16} W/g

10.3.3 Driver scenarios

The main task of the driver accelerator is to increase the kinetic energy and multiply the beam current extracted from the ion sources to the level of kiloamperes. The required current multiplication is dictated by the target physics and amounts to about 5 orders of magnitude. In the RF linac & storage ring scheme this is performed by a sequence of beam manipulations in the rings, following the acceleration in the RF linac. For the induction linac, acceleration and current compression always occur in a single structure such that the beam always stays close to the space charge limit according to its kinetic energy.

10.3.3.1 RF linac and storage ring systems

In the following we outline characteristic features of a driver satisfying similar requirements as in HIBALL [81Bad, 83Boc, 85Bad], but reduced to 3 MJ energy (instead of 10 MJ) to satisfy the needs of target ignition with an energy gain < 10. A schematic layout is shown in Fig. 10.7. This schematic representation is borrowed from the HIDIF study [98HID].

Linac: It has the task of providing a pulse of 10 GeV Bi^+ ions sufficiently long to fill all storage rings and thus accumulate the desired total energy. For a pulse current of 400 mA this requires about 1.5 ms to fill all accelerators for one fusion shot. At the low energy end many ion sources feed their current into parallel RFQ channels followed by drift tube linacs. Repeated funneling of two adjacent channels into one channel is done with simultaneous frequency doubling. This finally leads to a combination in the single main linac, which accelerates up to the full energy. The total length of the RF linac is estimated to 3.4 km. The relatively short time to fill the storage rings for one ignition gives sufficient flexibility for repeated shots at a repetition rate up to 50 Hz.

Storage rings: The linac beam is stacked in the horizontal phase space plane to fill each of the 12 storage rings with ions. The stacked beam leads to a stored energy of 250 kJ per storage ring. The ions fill the RF buckets such as to create 12 bunches each 250 ns long. Subsequently, the RF voltage is ramped to its maximum value to perform a fast rotation in synchrotron phase space, which leads to a pre-compression of the bunches to 120 ns at the time of extraction.

Final compression and focusing: An important task of the final transport is to remove the time difference of bunches in one ring by delay lines and to provide the voltage – here by means of induction bunchers – to achieve the final compression of the bunches to a duration of 6 ns as is required for the targets. For final focusing it was found convenient to use a matrix of superconducting quadrupole lenses and focus a whole bundle of beams on each one of the two converters. Target physics requires a spot radius of about 2 mm, which is a challenge to the design of the final focusing system. The demonstration of the feasibility of this transport, compression and focusing was shown in the HIDIF study (for more details see Fig. 10.8). A schematic view of the HIDIF target designed for illumination by two clusters of beams is given in Fig. 10.9.

The most important conclusion of the HIDIF study was to demonstrate in a detailed accelerator feasibility study that the requirements of inertial fusion can be met – both with respect to target ignition and

the repetition rate needed for commercial energy production. Although the HIDIF study was sufficiently detailed in a number of key issues, like injection into storage rings and the actual storage process as well as final beam transport, other questions like accelerator activation and vacuum have remained open. They are the subject of design studies which are carried out at GSI Darmstadt in the context of its new *"International Accelerator Facility FAIR"* [03Hen]. Besides its mission in the structure of nuclei and particles, this facility aims at using heavy ions to generate dense plasmas with similar techniques of beam accumulation, compression and focusing on a small target spot. It can be expected that the detailed design of this facility, and later its operation, will help clarify further important accelerator-related questions which have remained open in the HIDIF study.

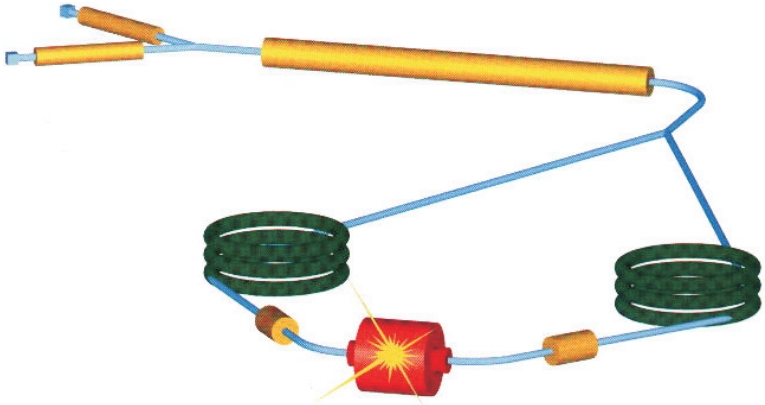

Fig. 10.7. Schematic layout of the HIDIF accelerator scenario.

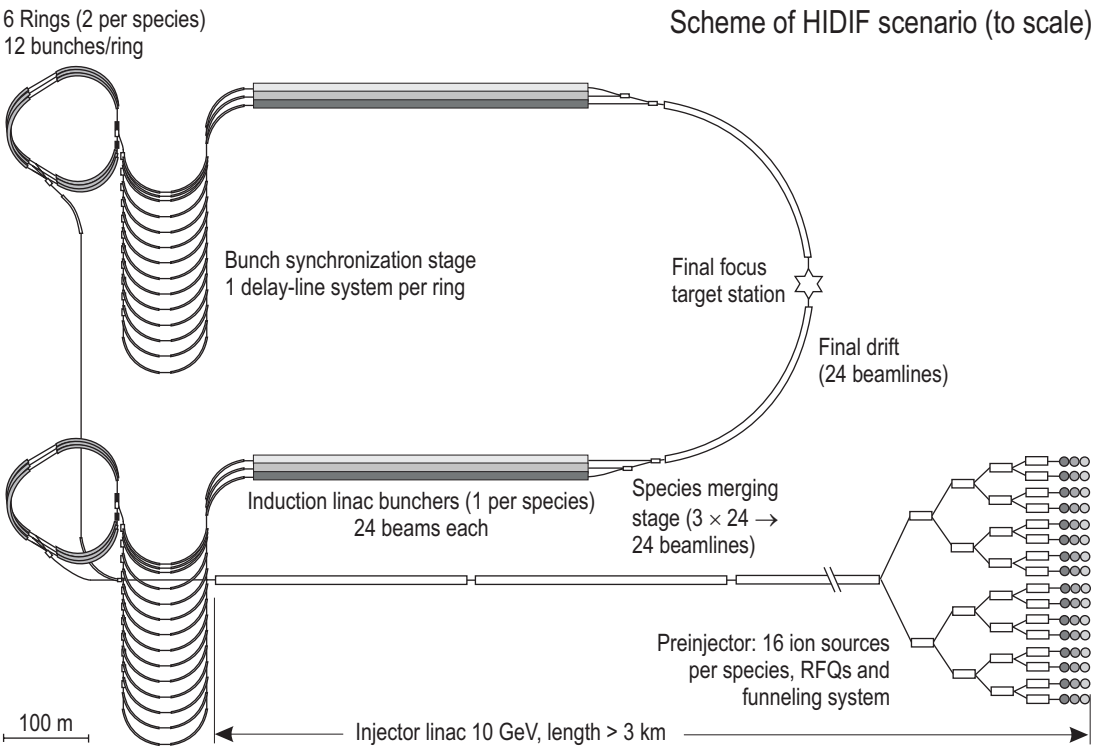

Fig. 10.8. Detailed layout of an RF linac & storage ring scenario.

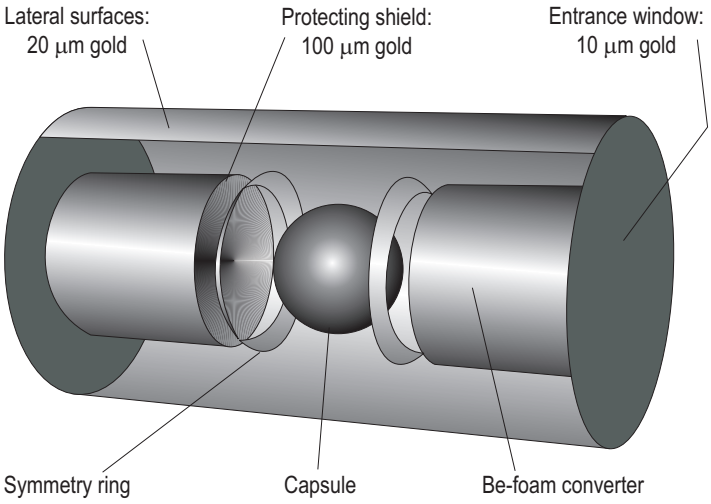

Fig. 10.9. Schematic view of HIDIF target designed for illumination by two clusters of beams (by courtesy of R. Ramis [98HID]).

10.3.3.2 Induction linac scenario and component development

In this section we give a more detailed account of the US Heavy Ion Driver Project pursued by the Virtual National Laboratory VNL, including LLNL Livermore, LBNL Berkeley, and Princeton University. The induction accelerator concept was first invented by Christofilos in the 1950s to accelerate high-current electron beams [64Chr]. The acceleration is achieved by the electrical field of ferromagnetic cores generated by induction on the axis of the beam line, as shown in Fig. 10.10. Solenoid magnets in drift spaces between acceleration gaps (not shown in the figure, for simplicity) provided radial confinement of electron beams. Subsequently, the induction accelerators ETA, ATA, and most recently DARHT [02Bur] have demonstrated peak beam currents up to 10 kA (ATA), 80 kJ/pulse (DARHT), and pulse repetition rates up to 5 kHz (ETA). With the demand for inertial fusion drivers the induction concept was applied to high-intensity heavy ion beams in the mid-1970s at LBL Berkeley [81Kee].

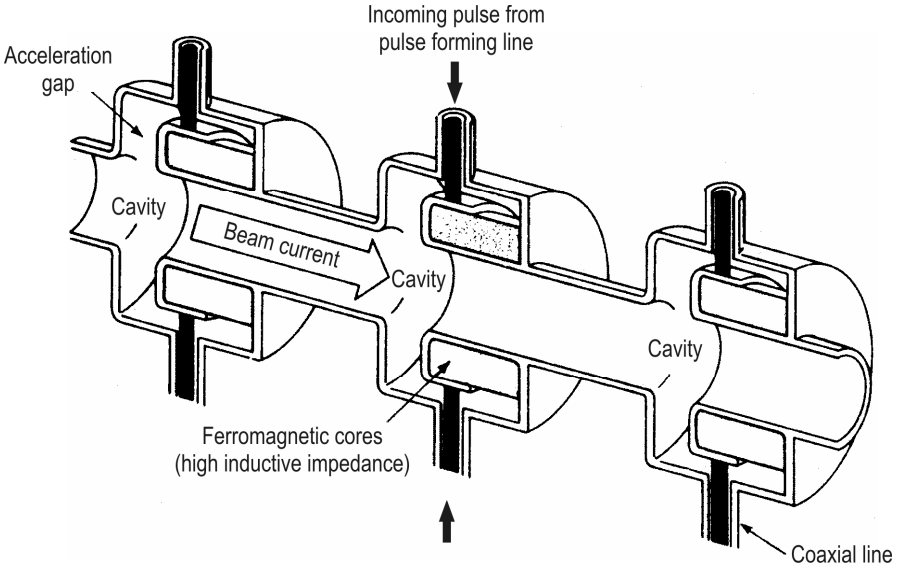

Fig. 10.10. Schematic cutaway of basic element of a linear induction accelerator.

Different from the RF linac funneling concept the induction linac is a single-pass accelerator consisting of many induction elements in series in which the heavy ion bunches are accelerated and – at the same time – longitudinally compressed. With proper low-impedance pulse forming lines driving the cores, the acceleration voltage can be maintained even with multi-kiloampere beam loading, and the beam bunch length can be compressed during acceleration for slightly relativistic ($\beta \approx 0.2$) heavy ion beams. The accelerator consisting of a large number of induction elements (as shown in Fig. 10.10) is preceded by a heavy ion beam injector and followed by a drift line in which the heavy ion bunches can be longitudinally compressed from several 100 ns bunches down to the 10 ns bunch needed to drive the fusion target. The overall scheme of a fusion driver is shown in Fig. 10.11. Useful power plant outputs of 1 GW (el) need several hundred MJ of fusion yield from targets injected at 4…8 Hz pulse rates. Accelerator electric-to-ion beam efficiencies > 25 % are expected.

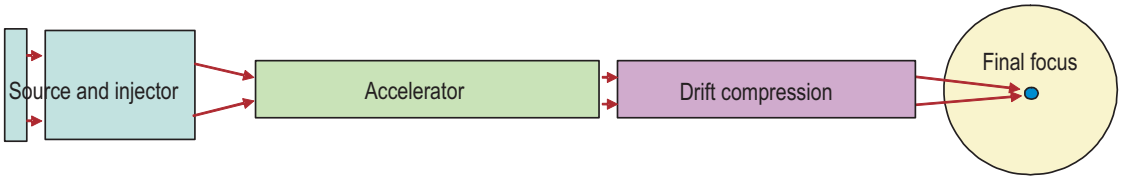

Fig. 10.11. Overall scheme of a heavy ion induction linac driving a fusion target.

Target requirements: Induction linac driver beam requirements come from considerations of IFE target requirements, efficiency and cost. Figure 10.12 shows typical US heavy ion target designs [99Cal, 00Cal] from which heavy ion beam requirements for induction linacs are derived. Because low-range ions (0.03 g/cm^2) are required to achieve symmetry and high gain for these targets, plasma neutralization of > 95 % of the beam space charge in the target chamber [02Wel] is required to focus the beams to the spot requirements of these target designs. Both the "Distributed-Radiator Target" (DRT) and the "Hybrid Target" (HT) designs shown in Fig. 10.12 require:

(1) Low-density beam-absorbing X-ray converter material distributed around a 5 mm radius hohlraum case for pressure balance and symmetry requires low-range (≈ 0.03 g/cm^2, $\beta \approx 0.2$) ions for target gain > 50.
(2) Smooth DT fuel capsules which absorb ≈ 1 MJ of soft X-ray drive energy to produce ≈ 400 MJ of fusion yield, giving a gain of ≈ 50. This requires a minimum accelerator efficiency (electrical to delivered beam) > 20 %.
(3) Enough beam directions (> 8 per beam end, depending on incident angles and spot overlap) for sufficient azimuthal symmetry.
(4) Pulse shaping with 20 % lower ion kinetic energy in the initial "foot" pulse to counter effects of range shortening on capsule drive symmetry.
(5) Plasma neutralization of > 95 % of the beam space charge in the target chamber.

Typical ranges of heavy ion target parameters are shown in Table 10.2. Figure 10.13 illustrates why chamber plasma neutralization is required for such low-range ion targets.

Table 10.2. Typical ranges of HIF target parameters.

Ion range	0.02…0.04 g/cm^2
Ion mass numbers, A	130…200
Ion energy, T_f	2.5…4 GeV
Total beam energy, E_d	6…8 MJ
Final pulse width, τ_f	8…9 ns (peak)

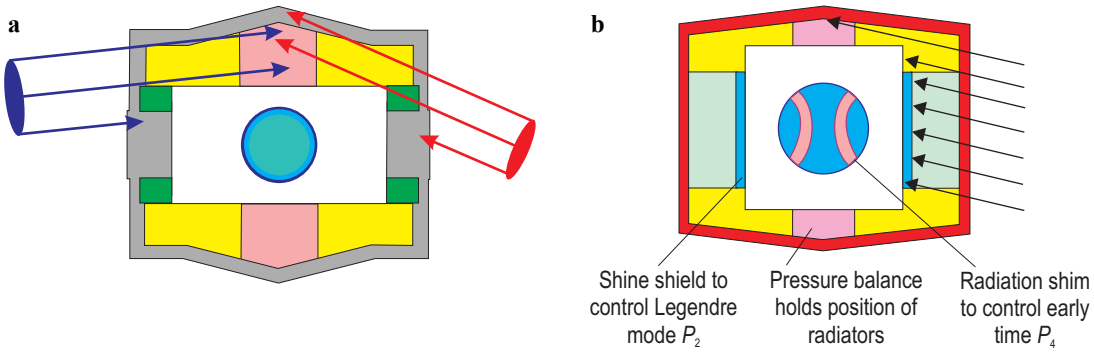

Fig. 10.12. **(a)** The Distributed-Radiator Target (DRT) for 120 beams up to 24° incident angle. **(b)** The Hybrid Target (HT) allows larger focal spot radii with fewer beam directions at smaller incident angles.

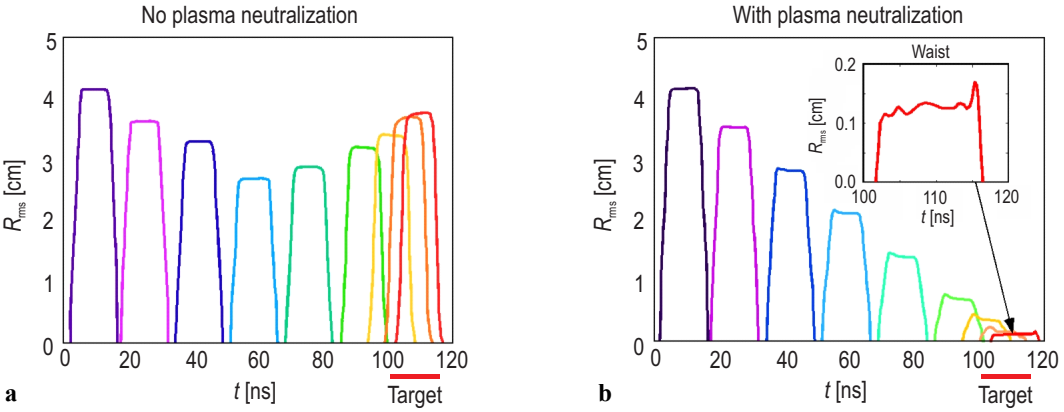

Fig. 10.13. PIC simulations [02Wel] of a 10 ns, 3 kA, 2.5 GeV Xe^{+1} beam ($\beta = 0.2$) focused at 10 mrad, **(a)** without, and **(b)** with pre-ionization of 1 mtorr molten-salt vapor in the target chamber. Ions strip up to +8 charge state over the 6 m focal length.

Transport. During acceleration and longitudinal bunch compression, the ion bunch must be confined against its space charge forces by applying focusing electric or magnetic fields. For induction linacs meeting the low-range ion target requirements described in Fig. 10.11, the space charge forces dominate over the transverse (emittance) pressure of the beam throughout the system, except where plasma neutralization removes the space charge, such as in the target chamber. Induction linacs can use two different types of focusing magnets, quadrupoles and solenoids, which can transport maximum beam currents I as functions of field B, average beam radius a, normalized "velocity" $\beta\gamma$, z-average magnetic field occupancy fraction η,

$$I_q = 8 \times 10^5 \, B_q \, a_q \, (\beta\gamma)^2 \, \eta_q \,, \tag{10.4}$$

$$I_s = 4 \times 10^5 \, (q/A) \, B_s^{\,2} \, a_s^{\,2} \, \beta\gamma \, \eta_s \,, \tag{10.5}$$

where the subscripts "q" and "s" are to distinguish parameters for magnetic quadrupole and solenoid transport, respectively. In (10.4) the value of the transverse quadrupole field, B_q, is the value at the pole tips: $1.25 \cdot a_q$ times the quadrupole radial field gradient. This approximate expression for alternating-gradient focusing assumes quadrupole lengths and spacing vary with beam energy along the linac so as to maintain a constant betatron wavelength per magnet (70° tune). Note the dependence of the solenoid transport current limit on ion charge to mass ratio, q/A, in (10.5), the faster dependence on $B \cdot a$, and the slower dependence on $\beta\gamma$, compared to quadrupoles. Thus, the average beam current density for quadrupole transport in an array increases for smaller beams until the quadrupole magnet winding thickness

becomes comparable to the space between beams, whereas for solenoids, the average current density increases with $B_s \cdot a_s$ until limits on B_s set by the superconductor current density or on beam space potential with a_s are reached. Because of the different scaling of the transport current between (10.4) and (10.5), the induction linac architecture with quadrupoles can have a large bundle of small beams transported together in an array within a common induction core, whereas for solenoids, the optimum beam size and current is large enough to permit the use of single-beam linacs accelerated with separate induction cores, to allow a modular approach for development.

Induction acceleration. For an average core azimuthal cross-section per meter of axial linac length of A_c (in m^2/m), the z-average acceleration gradient is $\langle E_z \rangle = A_c \Delta B/\tau_c$, with the maximum core flux swing ($\Delta B \approx 2.6$ T) in a period τ_c. Due to final induction-voltage rise and fall times, the "flat-top" part of the pulse useful for beam acceleration is about half of τ_c, i.e. the beam pulse width is $\tau_b \approx 0.5\,\tau_c$. Transport magnet support, vacuum pumping, and voltage-holding insulation typically require about 35 % of the axial space, while radial insulation between core material layers occupies 20 % of the radial build; thus, the effective packing fraction of core metal cross-section is limited to about 52 %. There is a variety of insulation options for induction cores, with a cost-effective limit about $\langle E_z \rangle_{max} \approx 1.5\ldots3$ MV/m. Each induction pulse with a flux swing ΔB incurs magnetic and eddy-current energy losses E_{lc} in the metal portion of core volume which increase with ΔB and with shorter pulses τ_c roughly according to:

$$E_{lc} = 3.8 \times 10^{-3}\, \Delta B^{2.7}\, \tau_c^{-0.7} \quad (\text{in J/m}^3)\,, \tag{10.6}$$

where E_{lc} given by (10.6) is an approximate fit over pulse widths τ_c ranging from 4 to 0.2 μs. Core losses increase more sharply than $\tau_c^{-0.7}$ for pulses shorter than 0.2 μs, putting cost and efficiency limits on the shortest $\tau_c > 0.1$ μs ($\tau_b = 50$ ns) for induction linacs using amorphous ferritic metal. The core energy losses per meter per pulse, $E_{lc}V_c$, equal the beam energy gain per meter, $\langle E_z \rangle N_b I_q \tau_c/2 = A_c \Delta B N_b I_q/2$, at about $\tau_c = 0.4\ldots0.2$ μs ($\tau_b = 0.2\ldots0.1$ μs). Assuming an electrical pulse-forming-line efficiency of $\eta_{pfl} = 0.75$, the local accelerator efficiency η_a (electrical input to beam output) would be $0.5\,\eta_{pfl} = 0.38$ at these pulse widths and currents.

Longitudinal bunch compression. Since the pulse widths for efficient induction acceleration are much longer than required for the pulses arriving at the target, induction linacs are designed to provide a few percent coherence velocity change in each bunch going from the front to the rear of each bunch, so that the bunches compress in a drift line of a few hundred meters length between the linac and the target. In addition to this drift compression, the bunch length L_b can also be compressed during acceleration, to maximize average beam currents and induction efficiency. Random voltage errors during beam injection, and crossing many induction acceleration gaps can generate a random momentum spread δp on each beam, which is multiplied by compression due to the "longitudinal invariant" conserving ($\delta p L_b$), leading to increased chromatic focusing aberrations. Studies [88Dud, 98Mei, 01Mei] indicate maximum injection bunch lengths L_{bm} should be limited to approximately < 60 times the final target bunch length L_{bf}.

Drift compression and final focus. Two-sided illumination hohlraum targets (see targets in Fig. 10.12) allow induction linac drivers to be used with chambers protected with thick-liquid flows. An example [03Yu] using arrays of molten-salt jets is shown in Figs. 10.15 to 10.17.

In the single multiple-beam quadrupole-focused linac case corresponding to [03Yu] the 120 beams are split into two groups and routed through the bends to the focusing arrays on both ends of the chamber as shown in Fig. 10.15. The beam must be longitudinally compressed by a factor of 22 during transport through ≈ 400 m of bends between the linac and the final focus in the reactor chamber. An ≈ 3 % velocity tilt head-to-tail is imposed by the last part of the linac such that the longitudinal beam space charge would remove the velocity tilt just before the compressed bunch arrives at the final focus. The final bunch current of 1.9 kA per beam for 4 GeV Bi^{+1} ions has too much space charge to focus to the required target spot size (see Fig. 10.13a) in a vacuum chamber with 1 ntorr of vapor, unless the vapor is pre-ionized (Fig. 10.13b).

Conclusions. Quadrupole- and solenoid-focused induction linacs are to be optimized to quite different beam parameters due to different transport limits, and the different beam parameters for each case are most suited for different targets and different compression and focusing regimes. Further R&D is needed to clarify how halo generation, beam loss, secondary electron ingress, and emittance growth might be

different because of the different field geometries in these two cases. All cases require pre-ionized plasma in the target chamber to remove most of the beam space-charge for existing low-ion-range target designs. Thus, beam-plasma interaction is a key R&D issue to enable either approach to induction linac drivers. The allowed accelerator emittance growth and longitudinal spread is very limited for 2 mm target focal spots, and both could be increased more than five-fold with hybrid targets (see Fig. 10.12b), making development of hybrid targets a high priority for induction linac drivers. Finally, as the cost of multiple-beam linacs has so far been a practical barrier to HIF development, the modular solenoid linac option may offer a lower-cost development path for HIF, in addition to lower-cost drivers.

10.4 The inertial fusion reactor

10.4.1 Introduction

The most specific feature of the *inertial fusion reactor* is the spatial separation of the reaction chamber from the driver facility. This separation offers much freedom for its conceptual design and opens excellent opportunities for technical solutions. In particular, it allows the realization of a thick fluid wall inside the reactor chamber which – by protecting the mechanical structures of the reactor chamber and of the final focusing system from neutron damage – will enable reactor lifetimes of more than 30 years without replacing the major structural components. At the same time, this fluid serves as a coolant, achieving the heat transfer to the conventional electricity-generating plant facilities, and as a breeder medium for the regeneration of tritium fuel. By such a design favorable properties can be realized with respect to safety, maintenance and economics, as pointed out in previous contributions. In this section we will concentrate on the specific features of the *heavy ion* driven inertial fusion reactor design which in many aspects are similar to the laser-driven reactor.

A number of reactor chamber concepts for a heavy ion beam driven power plant have been developed since the late 1970s, when the heavy ion accelerator was first considered as a driver for the inertial fusion reactor. In the early heavy ion reactor studies, such as HIBALL (1981, 1985) [81Bad, 83Boc, 85Bad], CASCADE (1982) [90Pit], and HIBLIC (1984) [84HIB], many problems for a conceptual design of a GW-size power reactor and for its operational requirements were investigated and innovative solutions proposed. Also the radiation damage and activation of materials as well as the economic viability of a heavy ion driven reactor have been addressed in the early 1980s. However, these designs were based on *direct drive* targets and on insufficient knowledge about symmetry requirements for target irradiation and implosion dynamics. In recent years significant progress has been made on our understanding of the physics of targets [98Lin, 04Atz], as well as on many other aspects of heavy ion fusion, requiring a much larger number of beams. Particularly the concept of indirectly driven targets has considerably affected the reactor design concepts.

In this presentation we will concentrate on some of the more recent heavy ion driven reactor designs, such as OSIRIS [92Mei], Prometheus-H [92Wag], HYLIFE II [94Moi], and RPD 2002 [03Yu, 03Bro, 03Lat, 03Pem]. OSIRIS and Prometheus-H were conceptual designs for a 1 GW (el) power plant driven by a heavy ion induction accelerator. Both design projects were ordered and funded by the US Dept. of Energy. They were carried out jointly by associations of US industrial companies, universities and National Laboratories in 1990-1992. HYLIFE II (LLNL, 1993) was based on an earlier design of a laser beam driven reactor (HYLIFE I, 1978) and was re-designed and adapted to a heavy ion driver in the early 1990s. The most recent design along these lines is RPD 2002, a self-consistent “Robust Point Design” for a 1 GW (el) power plant, driven by a heavy ion induction accelerator. Many design issues of RPD 2002 are based on previous work for HYLIFE II. Another novel reactor design – based on fast ignition – has been published recently by a Russian group [02Med].

10.4.2 Systems overview

We anticipate that many general issues of the fusion reactor have been discussed in previous chapters. Particularly the introductory Sect. 5.5 deals with specific design features and basic operational procedures of the inertial fusion reactor: The target is injected into a cylindrical reactor chamber at a repetition rate of about 5 Hz and, having reached the center of the chamber, it is ignited by a large number of heavy ion beam bunches. A total beam power of the order of 5…10 MJ necessary for igniting an indirectly driven target (Fig. 10.12) which is provided by a total of more than 100 bunches, impinging on the target simultaneously from two opposite directions. The length of the pulse-shaped bunches is of the order of 10 ns, and the beam transport through the chamber is based on beam neutralization and/or ballistic focusing. The chamber walls are protected from radiation by a thick fluid wall of molten salt in which the energy of the fusion neutrons is deposited and the breeding of tritium fuel is achieved. Among various materials proposed for this purpose, Flibe (Li_2BeF_4) and Flinabe ($LiNaBeF_4$) have been selected for the recent designs, because these chemical compounds are not combustible, have a very low solubility for tritium, a low activation rate and an extremely low vapor pressure at the operational temperatures (up to 650 °C for Flibe, and 400 °C for Flinabe). The heat is transported by the liquid blanket to the conventional electricity-generating facilities. A cross section of a reactor vessel is shown in the introduction (Sect. 5.5, Fig. 5.23) for the HYLIFE II design, and in Fig. 10.14 for OSIRIS. The following detailed description of the reactor components is based mainly on the RPD 2002 design which is the most recent and first self-consistent reactor design driven by 120 heavy ion beams. Some characteristic power plant parameters for RPD 2002 are given in Table 10.3 (this set of parameters may be compared to the parameters shown in Table 10.1 of Sect. 10.3.2.2).

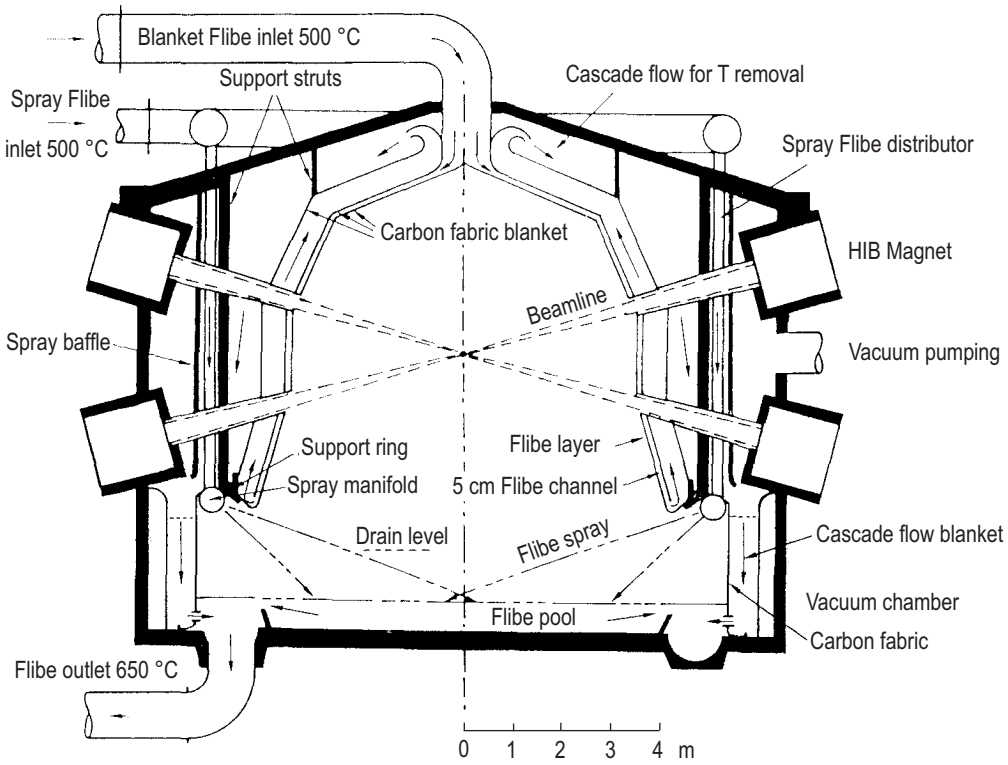

Fig. 10.14. The OSIRIS reactor chamber [92Mei].

Table 10.3. Summary of power plant parameters.

Driver energy per pulse	7 MJ
Target gain	57
Target yield	400 MJ
Pulse repetition rate	6 Hz
Driver efficiency	38 %
Fusion power	2400 MW
Thermal power	2832 MW
Conversion efficiency	44 %
Gross electric power	1246 MW
Auxiliary power	50 MW
Pumping power	27 MW
Driver power	110 MW
Net electric power	1058 MW
Driver cost	2.78 G$
Other plant cost	2.27 G$
Total plant cost	5.05 G$
Cost of electricity (COE)	7.18 ct/kWh

10.4.3 Reactor chamber design

10.4.3.1 Chamber and jet array system, clearing and condensation

A two-sided target illumination is used with beams arranged in 9×9 square arrays from two opposite directions, as illustrated schematically in Fig. 10.15, altogether 120 beams, 60 from each side. Flinabe is used as molten salt blanket for protecting the first structural wall from neutron and blast damage as well as for shielding the beam ports and the super-conducting final-focus magnets from radiation (Fig. 10.16). For this purpose, three primary types of liquid jets are used: Oscillating slabs, cylindrical jets, and annular vortex flows (Fig. 10.17). The oscillating jets are used to form a central pocket region where the target is injected and the micro-explosions occur. The beams enter this pocket through a high-precision square lattice formed by the cylindrical jets oriented at 45° from vertical. Scaled experiments using water have demonstrated that each of these three jet types can be created and can achieve the required smoothness. Many flow dynamical investigations and experimental studies have been performed for various geometrical arrangements of jets used in the different chamber designs (OSIRIS, HYLIFE II), taking also into account the neutron-induced isochoric heating of the blanket.

Several conditions must be considered in reactor design to allow for an operation at high repetition rate. Following the explosion of the target, the resulting Flinabe splash from the previous pulse must be cleared away to allow target injection and beam propagation through the chamber for the next shot. Different techniques have been investigated. Cold Flibe may be sprayed into the annular region between blanket and vessel wall at a rate that is capable of condensing all vapor. From a study of spray performance, flow rates and the location and numbers of spray heads have been determined to achieve sufficient condensation for a 6 Hz operation. Currently no experimental and theoretical basis exists to set the upper limit on possible repetition rates, even though the system economics would favor somewhat higher repetition rates.

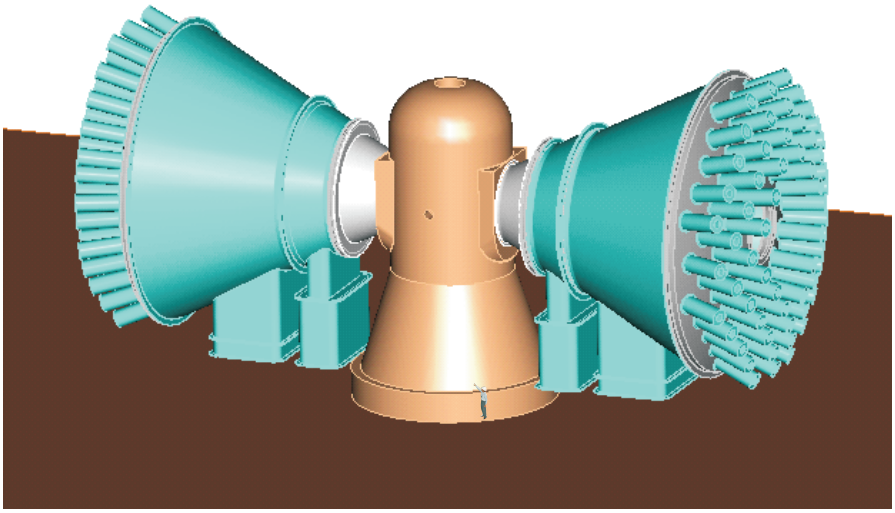

Fig. 10.15. An isometric view illustrating the coupling of final-focus magnet array with reactor chamber [03Bro]. (Courtesy of Wayne R. Meier).

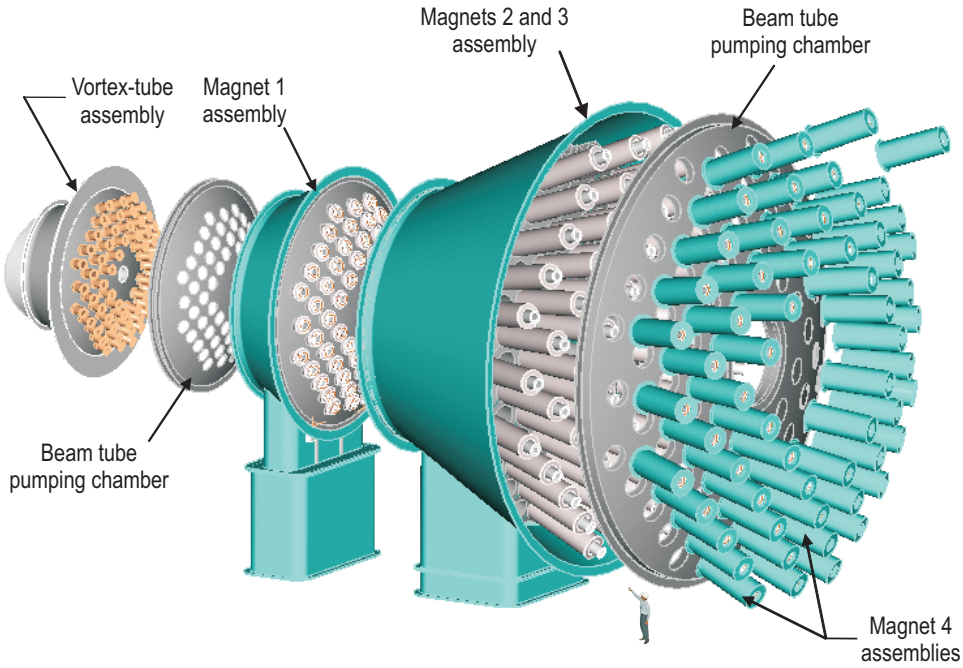

Fig. 10.16. Modular breakdown of final-focus magnets [03Bro]. (Courtesy of Wayne R. Meier).

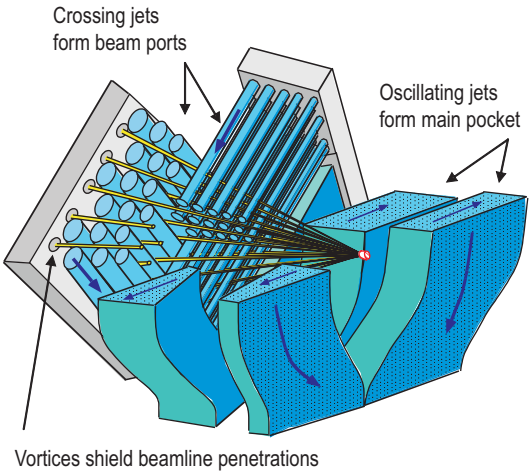

Fig. 10.17. Illustration of liquid jets required for the thick-liquid wall chamber [03Pem].

10.4.3.2 Target injection

Much work has been done for target design and for the development of target preparation techniques. The DT fuel is filled into the micro-shells by diffusion. Filling and layering techniques have been developed to prepare cryogenic fuel layers in the shells with the necessary high precision. These target fabrication techniques – being similar for all inertial fusion concepts – as well as the target factory have been developed mainly in the US [94Mon, 97Woo, 03Goo], but also in Russia [95Ale, 00Kor] and Japan [99Nor, 00Nor]. They will be described elsewhere.

The targets are injected horizontally into the pocket of the Flibe jet array. A helium gas gun is proposed to inject targets into the chamber. At a repetition rate of 6 Hz and a target velocity of 100 m/s it takes 30 ms of the 167 ms interpulse time until the target has passed to the center of the 3 m radius chamber. Target acceleration of 1000 m/s^2 (100 g) up to 100 m/s takes 100 ms and requires a 5 m long gun barrel. At this acceleration the cryogenic state of the fuel can be maintained during the whole injection process. About 10 mg of compressed helium is required to inject each target. The muzzle end of the injector is placed about 7 m from the chamber center to allow room for tracking the target with sensors.

10.4.3.3 Tritium technology and facilities

It is assumed that all the unburned tritium gas from the targets will be removed by the vacuum pumps on the reaction chamber. Tritium has low solubility in Flibe and tends to diffuse out, but the diffusion from thick-liquid jets is slower than the liquid's residence time in the chamber. A vacuum disengager has been designed to remove the breeded tritium from the molten salt. Two vacuum disengagers in series reduce the tritium concentration in the Flibe by a factor of 10^5 (Fig. 10.18). Only about 25 % of the *remaining* tritium permeates into the steam generator, so only about 10 Ci/day (much less than the allowable 40 Ci/day) will leak into the steam system.

10.4.3.4 Materials and molten-salt technology

For the vessel material and the pipes a "type 316" stainless steel will work with adequately low corrosion rate. Modified Hastelloy N (high-nickel steel) will work even better. Also the use of carbon-carbon composites for the vessel material has been investigated and will be considered for future concepts (OSIRIS). Graphite is compatible with the molten salt and would be satisfactory if tritium retention is not too serious. Pyrolytic graphite has low retention. The use of a Flibe-cooled graphite vessel will reduce activation, increase tritium breeding by reduced neutron absorption, and reduce heat leakage to the shield by absorbing neutrons more effectively. Some Flibe is ablated, vaporized, dissociated and ionized into its constituents by X-rays from the micro-explosion. Chemical kinetics of dissociated Flibe, however, indicates that

all these constituents will re-form Flibe and not other species, since recombination to Flibe is strongly favored. Recombination to Flibe is sufficiently fast compared with the timescales for the gas dynamics and condensation processes, so chemical equilibrium can be assumed. Based on investigations, it is predicted that all gas-phase chemical recombination processes are fast enough to maintain chemical equilibrium at pulse rates of 6 Hz and even much higher.

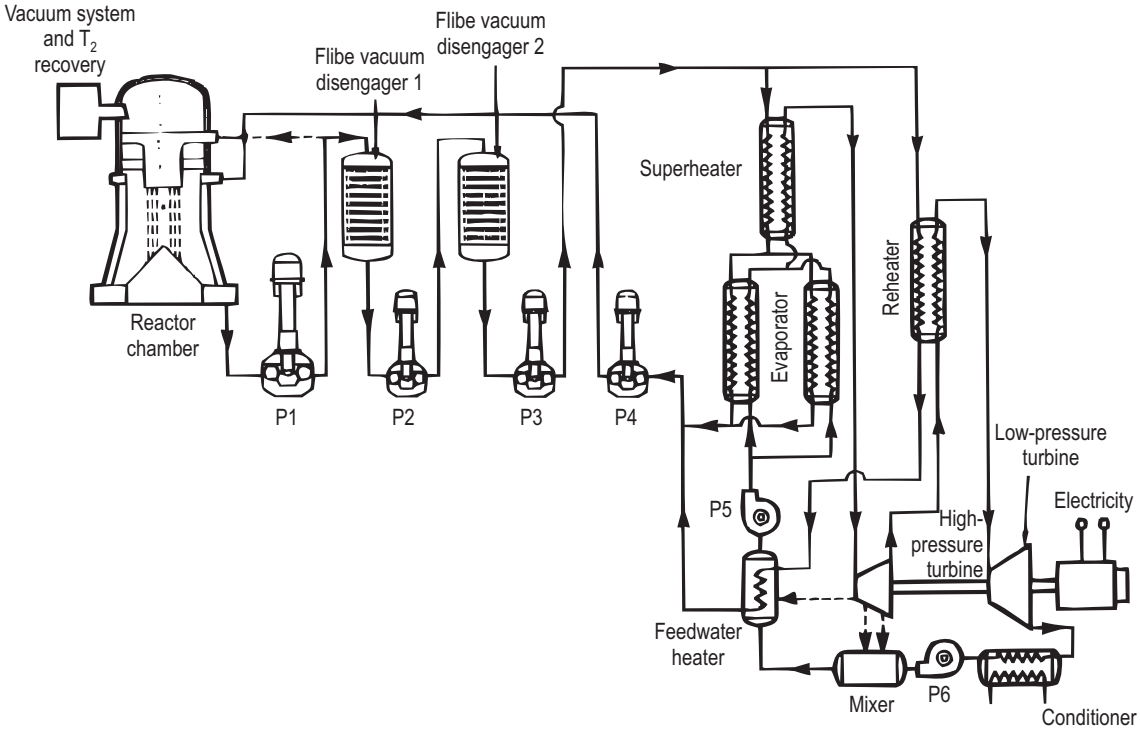

Fig. 10.18. Schematic of the HYLIFE II fusion power plant with a subcritical steam cycle; the Flibe vacuum disengager is shown on the left side, other components of the power plant on the right-hand side.

10.4.4 Neutronics and activation of materials, safety aspects

For HILIFE II and for other plant projects, detailed investigations on neutron flow, tritium breeding ratios, activation and radiation damage have been carried out. Neutronics analyses include the following areas: (1) The tritium breeding ratio is calculated to be 1.17 (15 % is bred in ^{7}Li, 85 % in ^{6}Li). (2) The energy released by nuclear reactions in the blanket, the target and chamber structures increases the fusion power by 18 % (system energy multiplication factor). (3) Radiation damage rates in terms of displacements per atom (dpa) and swelling by helium production have been calculated for various materials and turn out to be sufficiently low.

For the choice of first-wall material the primary issues are the compatibility with Flibe, the radiation damage and swelling resistance rates and the minimization of the long-term activation for disposal considerations. The liquid curtain allows neutron wall damage to be a secondary issue. In Fig. 10.19 the dpa for a 30-year operation is plotted as a function of the liquid-wall thickness [94Moi]. Type 316 stainless steel, for example, retains its strength up to a dpa of about 100. For Flibe this dpa value can be kept for a 30-year operation at a fluid-wall thickness of 56 cm. Without the protective Flibe layer, however, a dpa of 100 would be reached in only 1 year. (Prime candidate alloy is a modified version of type 316 SS which has better swelling resistance and is expected to exceed 100…150 dpa. Type 306 SS which shows lower acivation might be modified similarly. The goal of present design strategy is developing steel alloys with damage limit > 100 dpa and then show the effectiveness of thick-liquid wall in reducing dpa). Activation

studies for various materials were made to determine how much of the chamber would require deep burial on decommissioning. The SBI (Shallow Burial Index) can be greatly enhanced by the Flibe thickness and the choice of the chamber material, an obvious advantage of the inertial fusion chamber. Replacing some of the steel vessel components by graphite (carbon-carbon composites) could further reduce activation considerably, and consequently the amount of material requiring deep burial. Investigations were also carried out for other chamber materials.

One of the outstanding features of energy generation by thermonuclear fusion – and in particular a great benefit of the inertial fusion reactor – is its favorable safety characteristics. This has been discussed in Chap. 5. Here we emphasize the low activation rate of the reactor material (as compared to the fission reactor) which greatly facilitates maintenance and waste management. For comparison, the radioactivity produced in a 30-year operation time is plotted for the time after shutdown in Fig. 10.20 for a fusion reactor (CASCADE) in comparison with a fission reactor. The radioactive inventory of the fusion reactor is smaller by several orders of magnitude.

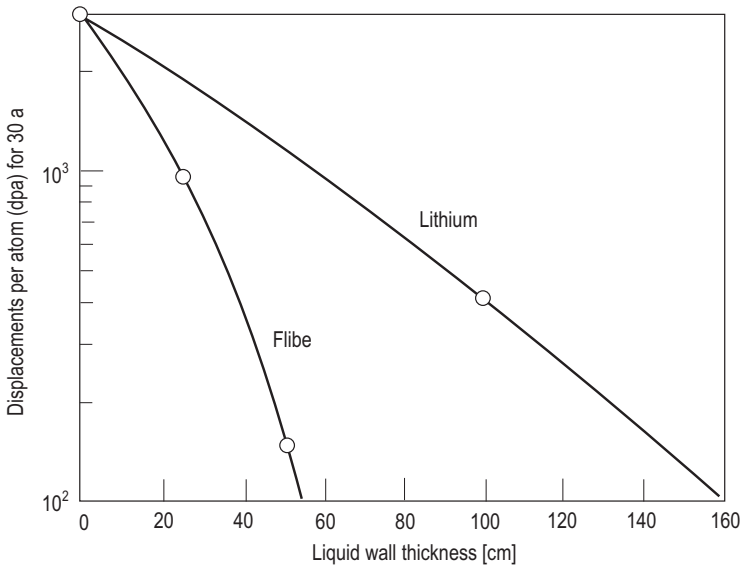

Fig. 10.19. Displacements per atom (dpa) for 30 years operation as a function of liquid wall thickness [94Moi]. A value of 100 dpa is an approximate limit for stainless steel. In magnetic fusion designs, the 100 dpa limit is reached in only 2 years. The curves are based on calculations for a radius of 3 m, 2700 MW fusion power, and 80 % capacity factor.

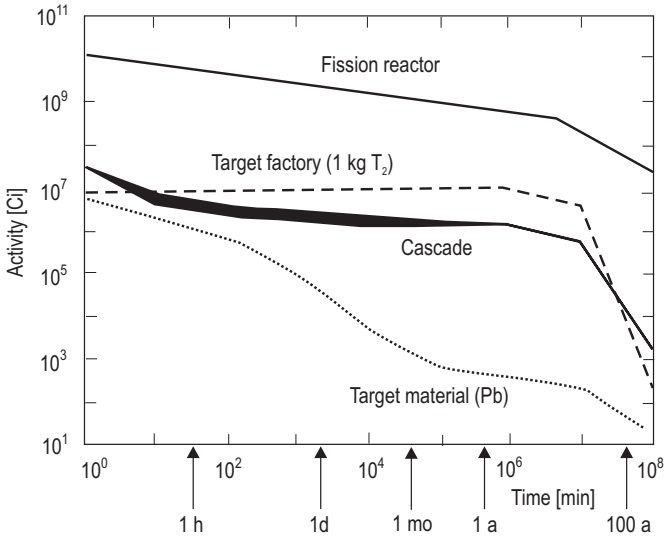

Fig. 10.20. Radioactivity of a 1 GW (el) fusion reactor (CASCADE [90Pit]) as a function of time after 30 years operation. Compared to the fission reactor it is, at any time, smaller by 3 orders of magnitude.

10.4.5 Power plant parameters and economic analysis

The cost of electricity (COE) is the most crucial parameter of a power plant with respect to its application for electricity generation. The investigation and analysis of COE, therefore, provides some guide lines for each conceptual design with respect to its efficiency. The aim of such investigations is primarily not the prediction of a precise figure of the COE for the time of operation in 30 years or so, but it is rather to get an assessment for the comparison of various designs, cost efficiency of improvements, comparison of various technologies. Also, the need for cost reductions in areas of expensive components or technologies needs to be investigated in terms of COE.

Since the cost of the driver is a major fraction of the total cost of the power plant, the driver capital and operational costs have to be fully included in the cost considerations, right from the beginning. For some of the investigated plant designs the cost analysis has been made without much variation and optimization of plant parameters ("point design"). In some cases systematic investigations have been carried out and systems analysis codes have been applied which allow a cost breakdown by varying the cost-effective parameters, such as the driver pulse energy and the pulse rate. In this context it should be mentioned, however, that some of the crucial parameters, such as the target gain, are assumed on the basis of theoretical predictions and have not been demonstrated yet by experiments. So, they have to be considered in such a cost analysis with caution.

In order to get a feeling about the crucial parameters, we follow here the parameter discussion and cost breakdown of RPD 2002, for which the parameters are nearly identical to those of the HYLIFE II design. Table 10.3 above summarizes the plant parameters for the RPD 2002, the "standard size" of a 1 GW (el) inertial fusion power plant. Assuming a driver pulse energy of 7 MJ and a (modest) gain of 57, the target yield per shot is 400 MJ. If the plant is operated at a repetition rate of 6 Hz, the fusion power produced is 2400 MW, and the total thermal power (including heat production by nuclear reactions) 2830 MW. With a thermal conversion efficiency of 44 %, the gross electrical power produced is 1246 MW. From this number the power consumption for the driver accelerator and for the various auxiliary facilities (pumping, target factory etc.) has to be reduced to get the net electric power of 1058 MW. To achieve this number the driver efficiency is assumed to be 38 % which might be somewhat too optimistic. On the other hand, some issues entering such cost estimates are derived from present-day cost estimates and could be further improved or optimized, e.g. the increase of repetition rate or target designs for higher gain. Since ignition has not yet been demonstrated, many basic assumptions for such an estimate are in a preliminary stage. But anyway, cost estimates provide useful and valuable guidelines for further improvements.

This situation is illustrated by the power flow diagram of a standard-size 1 GW power plant in Fig. 10.21. Taking into account the total cost of the plant of 5.05 G$ (2.78 G$ for the driver and 2.27 G$ for all other plant facilities), the resulting COE of 7.18 ct/kWh is very attractive. A comparison for the COE of different reactor and driver concepts and with other fusion power plants (inertial and magnetic confinement, some of them may be no more up to date) is shown in Fig. 10.22.

10.4.6 Conclusions

Considerable progress can be observed in heavy ion driven inertial fusion power plant design during the last decade. RPD 2002 is a major step forward, since more than twenty years ago with HIBALL a viable concept for target, chamber and driver had been jointly developed. Comparing the conceptual designs of HYLIFE II and RPD 2002, solutions have been worked out for many specific chamber issues, in particular the beamline/chamber interface, the shielded final-focusing concept, the first-wall shielding by an efficient jet system, demonstrated by scaled hydraulic experiments. Declassification of indirectly driven targets also has opened access to the performance of the most critical issue of the inertial fusion concept. For the most expensive facility, the heavy ion driver, two powerful options exist based on different technologies. These studies show the specific opportunities of the heavy ion driver concept, but they also exhibit issues and areas where future research is urgently needed or has to be intensified in ongoing programs.

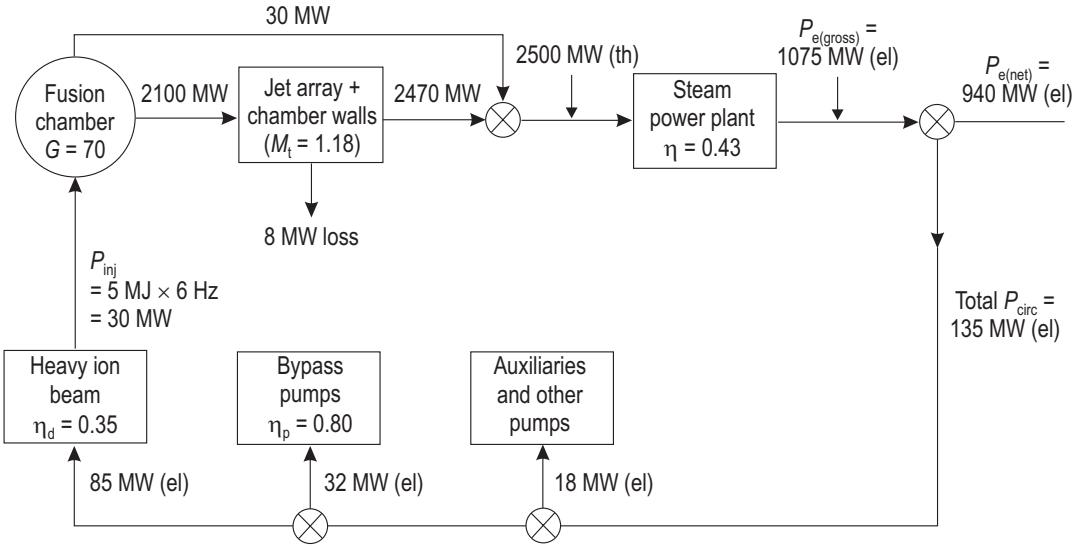

Fig. 10.21. Power flow diagram for the 940 MW (el) reference case.

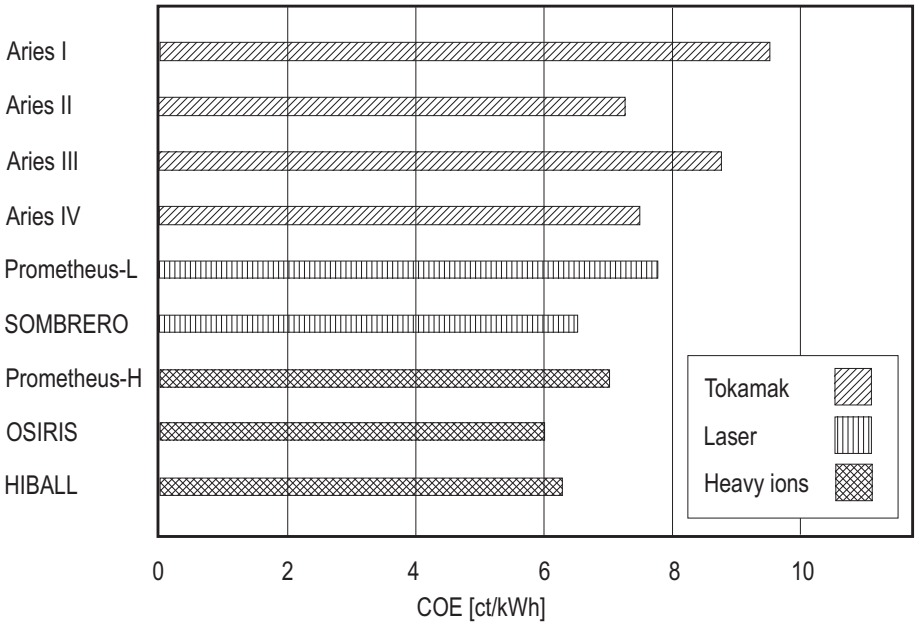

Fig. 10.22. Comparison of the cost of electricity (COE) for various fusion power reactor designs, both inertial and magnetic.

10.5 References for 10

64Chr Christofilos, N. et al.: Rev. Sci. Instruments **35** (1964) 886.

76Mas The first proposal of using high-energy accelerator technology for IFE goes back to A. Maschke and was presented at a workshop in 1976 in Oakland/California.

79Mas Maschke, A.W.: unpublished note (1979).

81Bad Badger, B. et al.: HIBALL, A Conceptual Heavy Ion Beam Driven Fusion Reactor Study, Kernforschungszentrum Karlsruhe, Report KfK 3202 (1981).

81Kee Keefe, D.: Research on High Beam-Current Accelerators, Particle Accelerators, Vol. 11 (1981) 197-199.

83Boc Bock, R., Böhne, D., Hofmann, I., Kessler, G., Kulcinski, G.L., Meyer-ter-Vehn, J., v. Möllendorf, U., Moses, G.A., Müller, R.W., Sviatoslavsky, I., Vogelsang, W.F.: IAEA Report TC392/29 (1983).

83Hof1 Hofmann, I., Laslett, J., Smith, L., Haber, I.: Particle Accel. **13** (1983) 145.

83Hof2 Hofmann, I.: Adv. Electron. Phys. Suppl. **13 C** (1983) 49.

84Chu Chupp, V. et al.: Proc. Internat. Symposium on Heavy Ion Accelerators and their Application to Inertial Fusion, Tokyo (1984) 160.

84HIB Heavy Ion Fusion Reactor HIBLIC-1, Institute of Plasma Physics, Nagoya University, Report IPPJ-663 (1984).

85Bad Badger, B. et al.: HIBALL II, An Improved Conceptual Heavy Ion Beam Driven Fusion Reactor, Kernforschungszentrum Karlsruhe, Report KfK 3840 (1985).

86Kee Keefe, D.: American Institute of Physics Conf. Proceedings **152** (1986) 63.

88Dud Dudziag, D.J., Taylor, W.W., Herrmannsfeldt, W.B.: Fusion Technology **13** No. 2 (1988).

88Ram Ramis, R., Honrubia, J., Ramirez, J., Meyer-ter-Vehn, J., Piriz, A.R., Sanz, J., Ibanez, L.F., Sanchez, M.M., de la Torre, M.: Nucl. Inst. Meth. **A 415** (1988) 93-97.

90Pit Pitts, J.H., Bourque, R.F., Hogan, W.J., Meier, W.R., Tobin, M.T.: The CASCADE Inertial Confinement Fusion Reactor Concept, LLNL Report UCRL-LR-104546 (1990).

92Mei Meier, W.R. (W.J. Schafer Associates) et al.: Osiris and Sombrero, Inertial Confinement Fusion Power Plant Designs, WJSA-92-01; DOE/ER/54100 (1992).

92Mey Meyer-ter-Vehn, J., Murakami, M.: Particle Accel. **37-38** (1992) 519.

92Wag Waganer, L.M. (McDonnell Douglas Aerospace) et al.: Inertial Fusion Energy Reactor Design Studies, Prometheus-L and Prometheus-H, DOE/ER/54101; MDC 92E0008, (1992).

93Lin Lindl, J.D.: Nuovo Cimento **106 A** (1993) 1467.

94Boc Bock, R.: Proc. of the EPS Conf. on Large Facilities in Physics, Lausanne (1994) 211.

94Hof Hoffmann, D.H.H., Jacoby, J., Laux, W., de Magistris, M., Boggasch, E., Spiller, P., Stöckl, C., Tauschwitz, A., Weyrich, K., Chabot, M. Gardes, D.: Energy loss of fast heavy ions in plasmas, Nucl. Inst. Meth. **B 90** (1994) 1.

94Moi Moir, R.W., Bieri, R.L., Chen, X.M., Dolan, T.J., Hoffman, M.A., House, P.A., Leber, R.L., Lee, J.D., Lee, Y.T., Liu, J.C., Longhurst, G.R., Meier, W.R., Peterson, P.F., Petzold, R.W., Schrock, V.E., Tobin, M.T., Williams W.H.: HYLIFE II: A molten-salt inertial fusion energy power plant design – Final Report, Fusion Technology **25** (1994) 5-25.

94Mon Monsler, M.J., Meier, W.R.: Automated Target Production for Inertial Fusion Energy, Fusion Technol. **26** (1994) 873-880.

94Tab Tabak, M. et al.: Phys. of Plasmas **1** (1994) 1626.

95Ale Alexandrova, I.V.: Lebedev Physical Institute, Report 39 (1995).

95Jac Jacoby, J., Hoffmann, D.H.H., Laux, W., Müller, R.W., Wahl, H., Weyrich, K., Boggasch, E., Heimrich, B., Stöckl, C., Wetzler, H., Miyamoto, S.: Stopping of Heavy Ions in a Hydrogen Plasma, Phys. Rev. Lett. **74** (1995) 1550.

96Puk Pukhov, A., Meyer-ter-Vehn, J.: Phys. Rev. Lett. **76** (1996) 3975; Phys. Rev. Lett. **79** (1997) 2686.

97Mar Maruhn, J.A., Kang, K.H.: Fusion Technology **31** (1997) 251-26.

97Woo Woodworth, J.G., Meier, W.R.: Target Production for Inertial Fusion Energy, Fusion Technol. **31** (1997) 280-290.
98HID HIDIF Study, European Study Group on Heavy Ion Driven Inertial Fusion, Eds. I. Hofmann and G. Plass, GSI Darmstadt, Report GSI-98-06 (1998).
98Lin Lindl, J.: Inertial Confinement Fusion, Springer-Verlag, New York (1998).
98Mei Meier, W., Bangerter, R., Faltens, A.: Nucl. Inst. and Meth. in Phys. Res. **A 415** (1998) 249.
98Mey Meyer-ter-Vehn, J., Pukhov, A., Atzeni, S.: Europhys. News **29** (1998) 219.
98PHE PHELIX, Petawatt High Energy Laser for Heavy Ion Experiments, GSI Darmstadt, Report GSI-98-10 (December 1998).
98Tab Tabak, M., Callahan-Miller, D.: Nucl. Inst. Meth. **A 415** (1998) 75-83.
99Cal Callahan-Miller, D.A., Tabak, M.: Nuclear Fusion **39** (1999) 883.
99Nor Fusion Technol. **35** (1999) 147.
99Vat Vatulin, V., Afamas'eva, V., Bazin, A., Ermolovich, V., Jidkov, N., Karepov, V., Kharitonov, A., Romanov, Yu., Shageliev, R., Skrypnik, S., Vasina, E., Vinokurov, O., Bock, R., Maruhn, J., Hoffmann, D.H.H.: Conf. Proc. IFSA 99, Eds. C. Labaune, W.J. Hogan, and K.A. Tanaka, Bordeaux (1999).
00Cal Callahan-Miller, D.A., Tabak, M.: Phys. Plasmas **7** (2000) 2083.
00Kor Koresheva, E.R. et al.: Proc. of the IAEA TC Meeting, Madrid (2000).
00Nor Norimatsu, T.: Proc. of the IAEA TC Meeting, Madrid (2000).
00Sna Snavely, R.A. et al.: Phys. Rev. Lett. **14** (2000) 2945.
01Hen Henning, W. et al.: An International Accelerator Facility for Beams of Ions and Antiprotons, Conceptual Design Report, GSI Darmstadt (2001).
01Mei Meier, W., Bangerter, R., Barnard, J.: Nucl. Inst. and Meth. in Phys. Res. **A 464** (2001) 433.
01Rot Roth, M. et al.: Fast ignition by intense laser-accelerated proton beams, Phys. Rev. Lett. **3** (2001) 436-439.
02Bas Basko, M.M., Churazov, M.D., Askenov, A.G.: Prospects of heavy ion fusion in cylindrical geometry, Laser and Particle Beams **20** (2002) 415.
02Bur Burns, M.J. et al.: LBNL Report 51136 (2002).
02Cal Callahan, D.A., Hermann, M.C., Tabak, M.: Progress in heavy ion target capsule and hohlraum design, Laser and Particle Beams **20** (2002) 405.
02Log Logan, G. et al.: Proc. of the 19th IAEA Conf., Lyon, Paper OV/3-4 (2002).
02Med Medin, S.A., Churazov, M.D., Koshkarev, D.G., Sharkov, B., Orlov, Yu.N., Suslin, V.M.: Evaluation of a power plant concept for Fast Ignition Heavy Ion Fusion, Laser and Particle Beams **20** (2002) 419.
02Wel Welch, D.R. et al.: Physics of Plasmas **9** (2002) 2344.
02Yam Yamazaki, Y.: Proc. of the 2002 European Accelerator Conference, Paris (2002), p. 174.
03Bro Brown, T., Sabbi, G.L., Bernard, J.J., Heitzenroeder, P., Chun, J., Schmidt, J., Yu, S.S., Peterson, P.F., Abbott, R.P., Callahan, D.A., Latkowski, J.F., Logan, B.G., Meier, W.R., Pemberton, S.J., Rose, D.V., Sharp, W.M., Welch, D.R.: An integrated mechanical design concept for the final focusing region for an IFE reactor concept, Fusion Science and Technology (2003).
03Goo Goodin, D.T., Nobile, A., Hoffer, J., Nikroo, A., Besenbruch, G.E., Brown, L.C., Maxwell, J.L., Meier, W.R., Norimatsu, T., Pulsifer, J., Rickman, W.S., Steckle, W., Tillack, M.: Addressing the Issues of Target Fabrication and Injection for Inertial Fusion Energy, Fusion Engineering and Design **69** (2003) 4.
03Hen Henning, W.: Proc. of the 2003 Particle Accelerator Conf., Portland, USA (2003) 16.
03Hol Holtkamp, N.: Proc. of the 2003 Particle Accelerator Conference, Portland, USA (2003) 11.
03Lat Latkowski, J.F., Meier, W.R.: Shielding of the final focusing system in the robust point design, Fusion Science and Technology (2003).
03Pem Pemberton, S.J., Abbott, R.P., Peterson, P.F.: Thick liquid blanket configuration and the response for the HIF point design, Fusion Science and Technology (2003).

03Yu Yu, S.S., Meier, W.R., Abbott, R.P., Bernard, J.J., Brown, T., Callahan, D.A., Heitzenroeder, P., Latkowski, J.F., Logan, B.G., Pemberton, S.J., Rose, D.V., Sabbi, G.L., Sharp, W.M., Welch, D.R.: An updated point design for heavy ion fusion, Fusion Science and Technology (2003).

04Atz Atzeni, S., Meyer-ter-Vehn, J.: Physics of Inertial Confinement Fusion and High Energy Density in Matter, Clarendon Press, Oxford (2004).